NASA-CR-205016

MCR-96-1303, Issue 03

Contract Number: NAS8-40633

Membrane Transport Phenomena (MTP)

Semi-Annual
Technical Progress Report

November 1996 - May 1997

Principal Investigator, Program Manager:
Larry W. Mason

Prepared By:
Lockheed Martin Astronautics Company
Flight Systems Division
P.O. Box 179
Denver, CO 80201

Prepared For:
National Aeronautics and Space Administration
George C. Marshall Space Flight Center
Marshall Space Flight Center, AL 35812

LOCKHEED MARTIN

Table of Contents

MTP PROJECT ACTIVITIES

The third semi-annual period of the MTP project has been involved with performing experiments using the Membrane Transport Apparatus (MTA), development of analysis techniques for the experiment results, analytical modeling of the osmotic transport phenomena, and completion of a DC-9 microgravity flight to test candidate fluid cell geometry's. The MTA Fluid Profile Refractometer New Technology Report submitted with the last MTP semi-annual report (Nov. 1996) was selected for publication in NASA Tech Briefs. Preparations were also made for the MTP Science Concept Review (SCR), held on 13 June 1997 at Lockheed Martin Astronautics in Denver. These activities are detailed in following sections.

MTA DEVELOPMENT ACTIVITIES

The fluid valves used for controlling fluid flow in the MTA showed some problems, as described in prior technical reports. The Neoprene seat material used in these valves apparently has an affinity for water, and swells when in continuous contact with an aqueous solution. The swelling of the seat material may cause the valve to stick in the unactuated position, and consequently it will not respond to the control signals generated by the Fluid Manipulation System. The valve may also not seat completely, causing a leak within the MTA fluid cell. This has the consequence of altering the fluid flow data collected by the Volumetric Flow Sensors.

The Neoprene valves in MTA were replaced with new valves having Teflon seats. The valve cabling and wiring interface was also improved to facilitate the valve changeout. These new valves have worked well, and show no adverse effects from continuous contact with the aqueous solutions.

MTA REFRACTOMETER CALIBRATION

A calibration procedure was developed and implemented for the MTA Optical Refractometer. The procedure consists of layering a series of solutions having known refractive indices into both of the MTA Fluids Optical Cells (FOC), and acquiring the imaged profiles for a series of optical configurations. The images are analyzed using the image processing software, and evaluated to produce coefficients that relate the imaged refractive index profile (offset distance) to the known refractive indices through the geometrical configuration of the refractometer. Software was developed to implement this analysis, and to produce calibration coefficients for refractive index predictions based on the MTA optical geometry and imaged profiles.

The optical calibration is valid as long as the fluid cell assembly is not disturbed within the support frame, as happens when the assembly is taken apart to replace a membrane or repair a leak. Disassembly alters the optical geometry of the fluid cells relative to the incident laser, the membrane, and to the other fluid cell. The calibration is performed simultaneously on both of the two fluid cells (Upper & Lower). The MTA is first assembled complete with membrane and support grids in a leak free configuration within the support frame. The fluid cell support frame is then securely attached to the optical mount in the MTA instrument, and leveled. Care is taken not to minimize vibrations and disturbances to the assembly during the subsequent calibration activities.

Three fluid layers of known refractive index are carefully introduced into the FOC's (three layers in each fluid cell). The fluid in the lower FOC does not contact the membrane to

avoid osmosis and the associated mixing of the fluid layers. The peristaltic pumps are used to deliver about 7 cc fluid volume into each of the layers, in each of the fluid cells. The pumping rate is set very low (~.05 cc/sec) to minimize fluid turbulence during these filling operations. The fluid tubing is purged between the fluid layers to minimize the mixing between solutions and layers.

Once the calibration solutions are in place, calibration images are acquired for a series of refractometer geometry's. There are the two primary variables in the refractometer geometry: (1) MTA Rotation Angle (Theta) and (2) Projection Distance. Theta defines the laser beam incidence angle relative to the fluid cell, and the projection distance is a measure of the distance the refracted beam travels to the projection screen. Figure 1 shows a schematic of the MTA refractometer, and how these two variables affect the optical geometry.

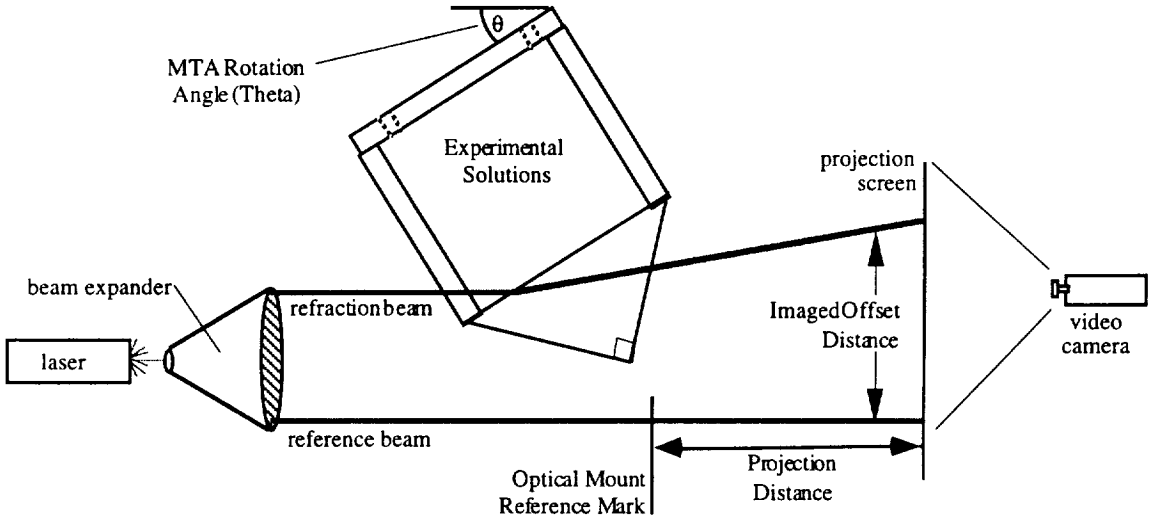

Figure 1 MTA Refractometer Schematic Diagram and Calibration Variables

Calibration data is acquired as a series of refractive index profile images with the MTA geometry varied to cover an operational range of parameters. The rotation angle (Theta) is set using the rotary table on the optical platform, and images acquired for a series of projection distances as set on the MTA optical rail. In this way, each of the geometrical variables is systematically varied, and images obtained for configurations that span the refractometer parameter space. The projection distance is measured from a reference mark on the optical platform, and is only an approximate value. The precise projection distance associated with each rotation angle is determined in the calibration analysis.

The images of the layered calibration solutions were subjected to image analysis to measure the imaged offset distance relative to the reference beam. This analysis produces data pairs that correspond to each pixel in the refraction beam image, relating the refraction offset distance to the fixed coordinate system provided by the membrane. Figure 2 shows data acquired during calibration of the refractometer at a fixed rotation angle (26°) for various projection distances.

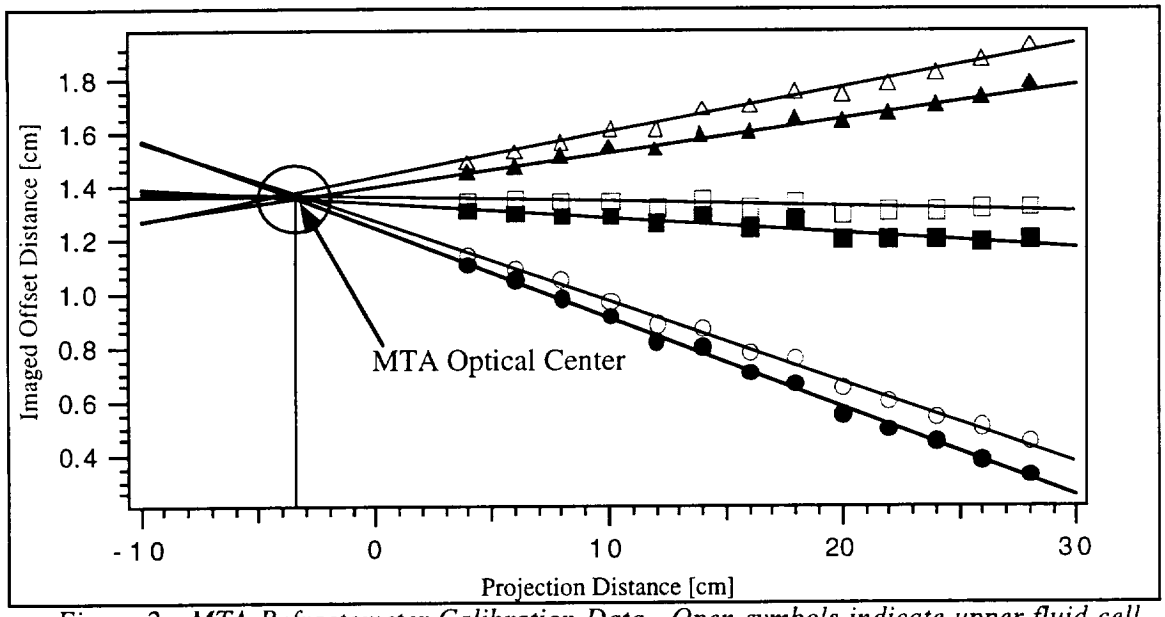

Figure 2 MTA Refractometer Calibration Data. Open symbols indicate upper fluid cell, closed symbols indicate lower fluid cell

The upper and lower fluid cells must be calibrated separately because they are separate and distinct units that differ slightly in construction and alignment within the support frame. The data show that the imaged offset distances converge to a point in the apparatus that has been termed the MTA Optical Center. This location in the MTA represents the point where the refraction beam exits the optical cell assembly. Knowledge of the optical center allows exact calculation of the projection distance and the offset of the refraction beam relative to the reference beam.

Figure 3 shows a schematic diagram of the geometry, and how the optical center is used to calculate the refraction angle for each of the calibration solutions present within the fluid optical cells. The optical center is used to determine the angle of the refraction beam upon exiting from the fluid cell. This angle (alpha) is computed as the inverse tangent of the opposite over adjacent legs (b/a) of the right triangle formed by the projection distance and the imaged offset.

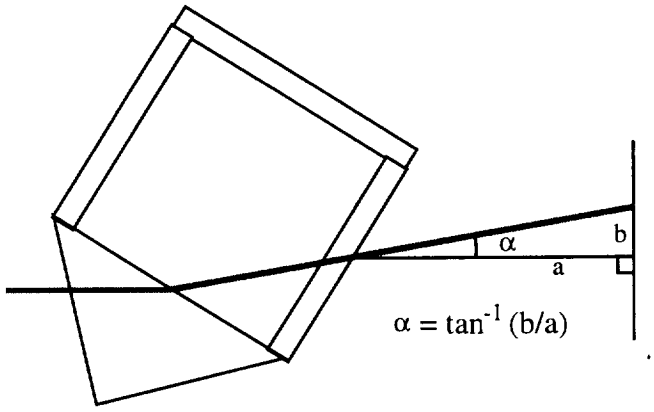

Figure 3 Fluid Profile Refraction Angle Determination

The refractive index of the solution present at any point within the fluid cell can be determined once the refraction angle is known. Figure 4 shows that the refraction angle is a linear function of the solution refractive index for the calibration solutions used.

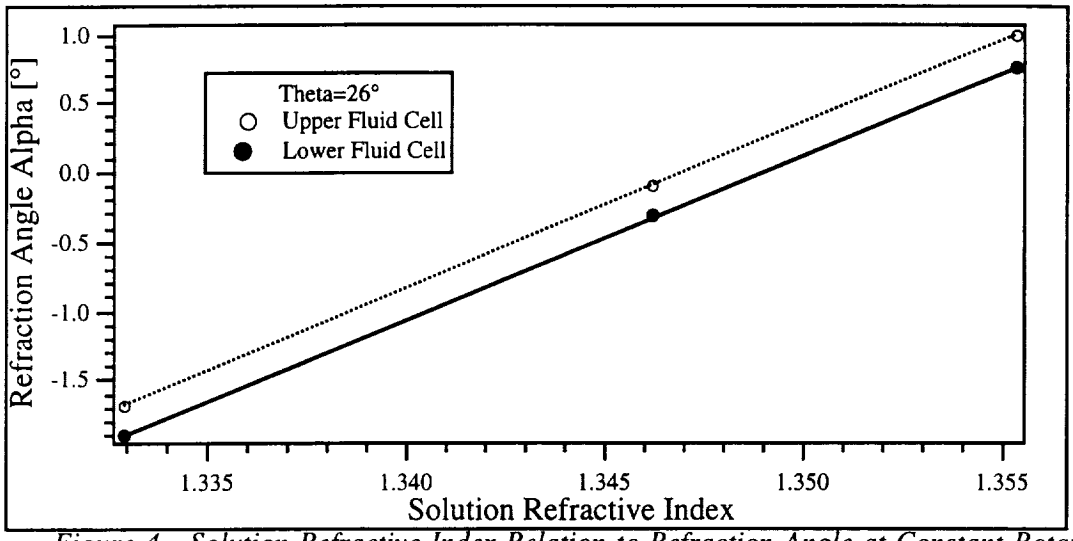

Figure 4 Solution Refractive Index Relation to Refraction Angle at Constant Rotation

The calibration of the refractometer is verified by comparing the measured solution indices of refraction to the index of refraction predicted by the Fluid Profile Refractometer. Figure 5 shows a plot of the calibration solution profile data at a constant rotation angle and projection distance.

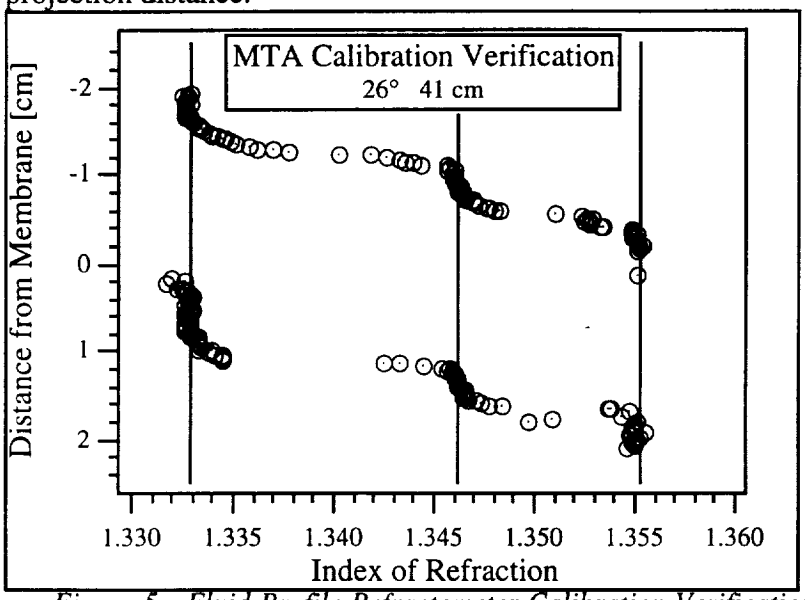

Figure 5 Fluid Profile Refractometer Calibration Verification

Each data point (open circle) represents one pixel in the refractometer image, and the vertical lines indicate the measured index of refraction for each of the calibration solutions. The membrane is present at the zero location on the y-axis, separating the upper and lower fluid cells. The measured and predicted refractive indices show high correlation.

OSMOSIS EXPERIMENT DATA ANALYSIS

Data analysis software was developed for the fluid profile refractometer images to enable all refractive index profiles obtained in an experiment to be summarized in a single three dimensional plot. This analysis provides an overview of each single experiment in terms of the development of the fluid boundary layer structure that forms in association with the membrane. The three dimensional plot details the fluid density as a function of distance from the membrane and experiment elapsed time. The fluid density is shown as contours that represent lines of constant fluid density. The individual images from the Fluid Profile Refractometer are analyzed and processed to produce data for fluid density as a function of distance from the membrane, with each image a snapshot in time of the boundary layer structure. Figure 6 summarizes how individual refractometer images are combined to generate an experiment overview and allow visualization of the fluid boundary layer structure development over time.

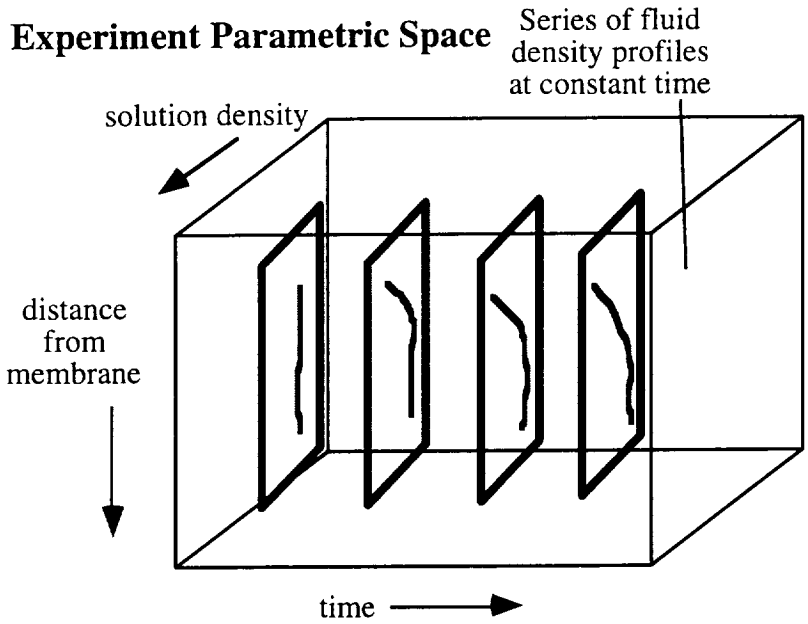

Figure 6 Integration of Fluid Profile Refractometer Images in Experiment Parametric Space Defined by Distance From Membrane and Elapsed Time

MTA OSMOSIS EXPERIMENTS

The Membrane Transport Apparatus (MTA) has been in almost continuous use, performing osmosis experiments using solutes over a wide range of molecular weights. The instrument has functioned well, and a comprehensive dataset has been generated. The dataset documents the effects of gravimetric orientation and solute molecular weight on the kinetics of osmotic transport, and the fluid boundary layer structure that forms in association with the membrane.

Each osmosis experiment consists of preparing and characterizing solutions, configuring the Membrane Transport Apparatus (MTA), transferring the solutions into the MTA fluid cells, and initiating the data acquisition software. Data is then acquired to document the kinetics of mass flow through the membrane and the boundary structure over time.

The experiment solutions are characterized in terms of: (1) mass of anhydrous solute, (2) total solution mass, (3) mass of known volume of solution, and (4) solution refractive index. A Mettler PM2000 analytical balance was used for all mass measurements. The balance measures to a precision of 10 mg, and is in an annual calibration cycle. Refractive index measurements were performed using a Leika 0-30° Brix hand-held refractometer. All measurements and experiments were performed under ambient (room temperature) conditions. Solute molecular weights were taken from manufacturers specifications and Material Safety Data Sheets (MSDS). The solution measurements were used to derive various solution properties and characterize the initial experiment conditions. The derived parameters include: (1) solution weight percent (w/w), (2) solution concentration (Molar), and (3) solution density (g/cm^3). Figure 7 shows a diagram of the measurements taken and the formulas used to derive the solution characteristics.

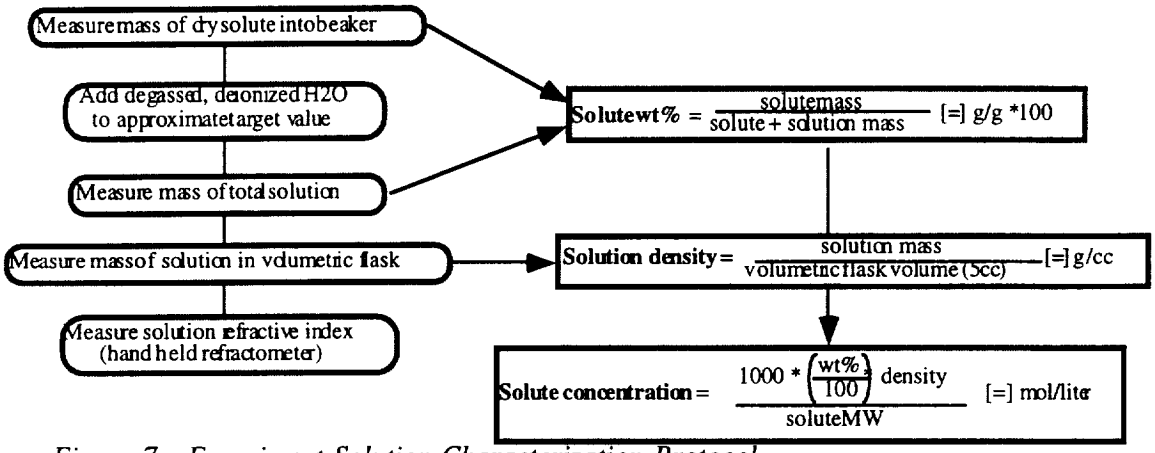

Figure 7 Experiment Solution Characterization Protocol

The solution parameters measured using this procedure are related to one another. Figure 8 shows some of these relations as measured for sucrose.

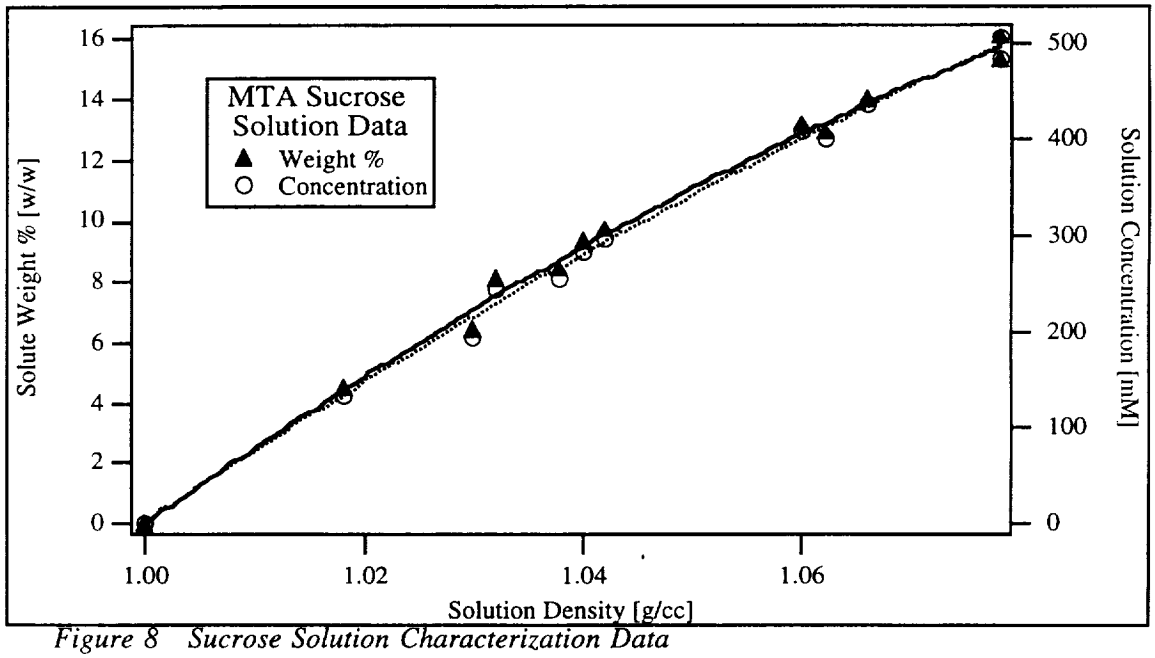

Figure 8 Sucrose Solution Characterization Data

Each data point represents a single solution that was characterized, and the lines represent a second order polynomial fit to the data. These relations are used in analysis of the experimental data to convert the refractive index profiles into fluid structure data in appropriate units (solution density, concentration, mole fraction, etc.).

Once an experiment solution has been prepared and characterized, it is transferred to either the Upper or Lower Fluid Optical Cell (FOC) using the Fluid Manipulation System, depending on the gravity vector orientation of the experiment. Deionized water is transferred into the opposite FOC to initiate the experiment. The current fluid cell design is not yet optimized for fluid filling and draining operations, and manual manipulation of the fluid cell assembly is required to insure that complete filling occurs (no trapped bubbles). The initial conditions of an experiment correspond to the MTA maximum hydrostatic pressure across the membrane, and maximum membrane pillowing in one direction. This configuration sets the membrane in an initially rigid position. As osmosis drives water through the membrane, the relative levels in the Volumetric Flow Sensors change, and are recorded as experimental data along with the ambient temperature. Refractive Index profile images are also acquired at regular intervals over the course of the experiment. The changing fluid levels in the fluid cells cause the hydrostatic pressure present across the membrane to change over time, and can cause movement of the membrane as the experiment proceeds.

Osmosis experiments have been performed using solutes over a wide range of molecular weights. Figure 9 shows an overview of the solutes and initial concentrations used in these experiments. Each data point represents a single experiment with the (log) solute molecular weight plotted on the x-axis, and the experiment solution initial concentration plotted on the y-axis. The decreasing concentration trend shown in this figure is a consequence of the increasing solute molecular weight, and solution solubility limits.

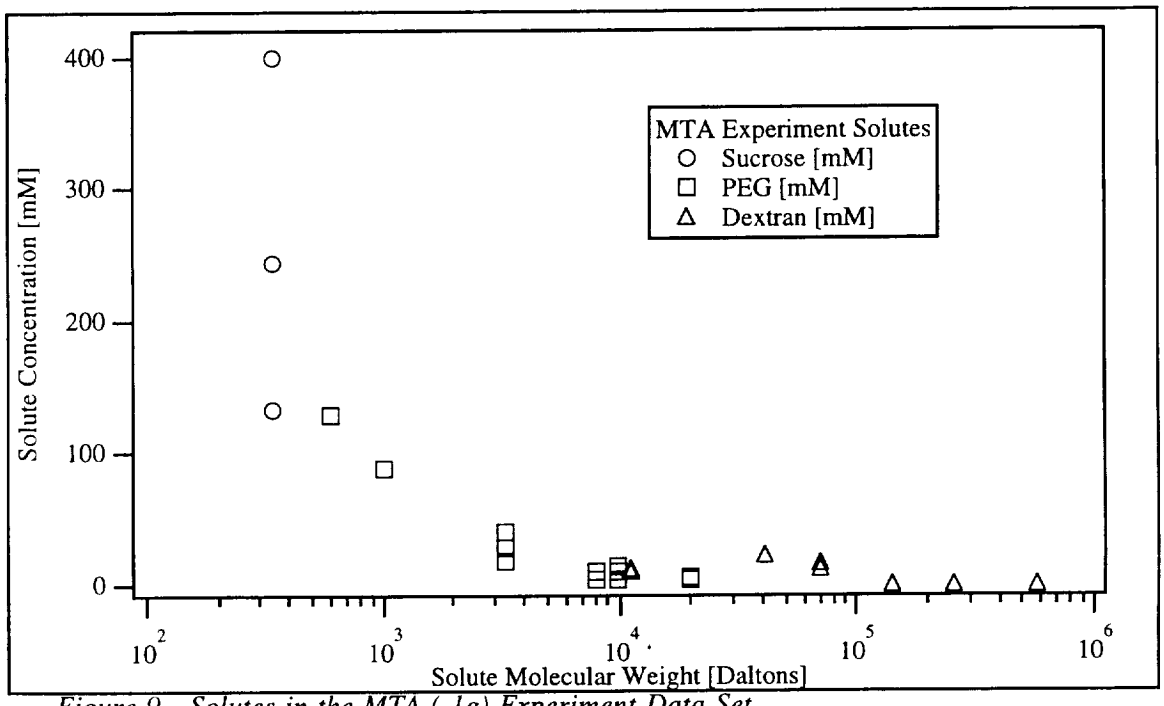

Figure 9 Solutes in the MTA (-1g) Experiment Data Set

Two orientations of the experiment fluids with respect to gravity were used for these experiments. A convention was adopted for these two orientations: (+1g) to indicate the solution located physically on top, and (-1g) to indicate the solution present in the lower fluid cell.

Results From Solute on Top (+1g) Gravimetric Configuration

In this configuration, the osmotic solution is present in the upper fluid cell. Osmosis causes lower density solvent (DI water) to pass through the membrane into the higher density solution from the bottom, and a density inversion is created in the solution. Gravity driven buoyancy driven convection occurs causing the solution to mix. The mixing action functions to continually present fresh solution to the membrane surface, and drive the osmosis process. In all of the experiments performed in this configuration the refractometer images showed no change as the experiment proceeded, indicating that the solution fluid cell was mixed during the experiment. Figure 10 shows raw data from the Volumetric Flow Sensors for the (+1g) configuration.

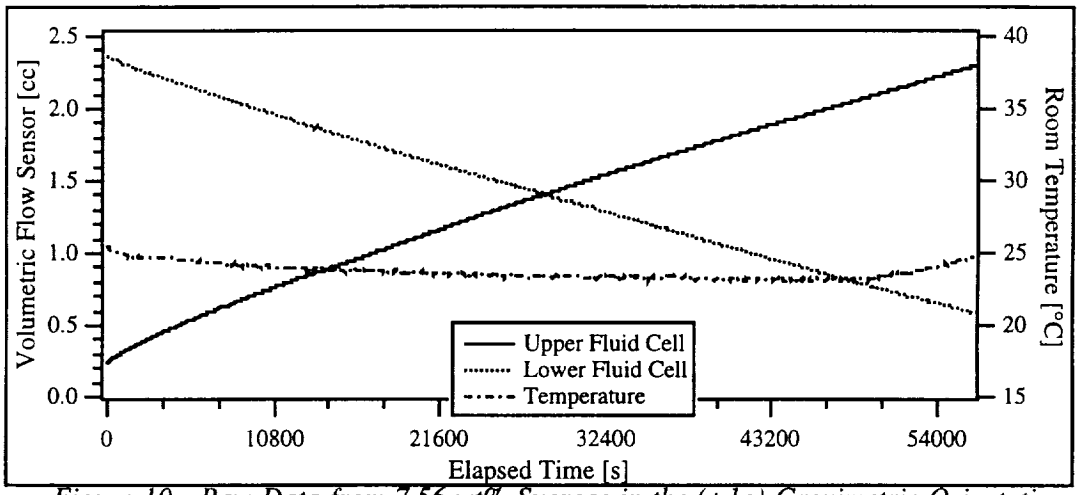

Figure 10 Raw Data from 7.56 wt% Sucrose in the (+1g) Gravimetric Orientation

Differentiation of the volumetric flow data with respect to time results in data having units of cc/s, or volumetric flow rate. Figure 11 shows the differentiated volumetric flow for 7.56 wt% sucrose solution in the (+1g) configuration.

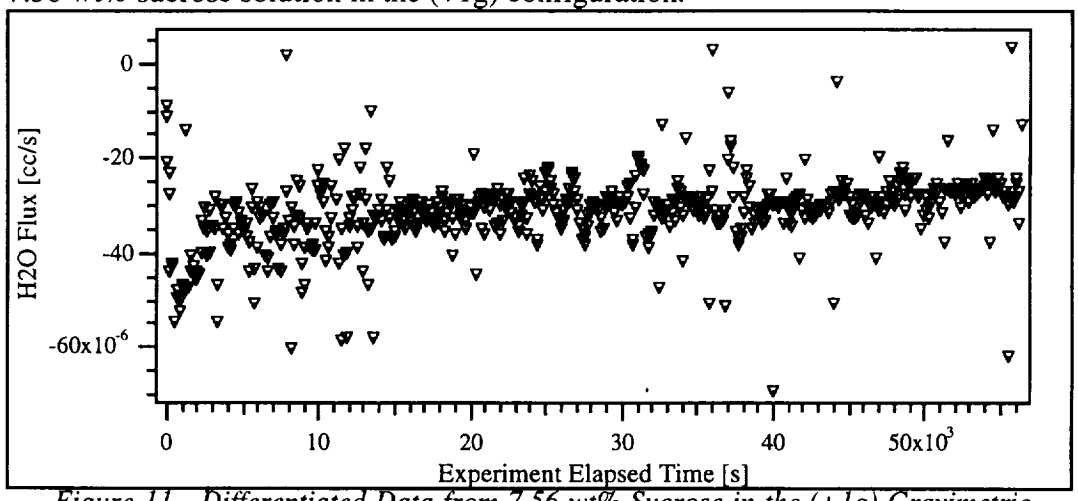

Figure 11 Differentiated Data from 7.56 wt% Sucrose in the (+1g) Gravimetric Orientation

The data can be further processed by dividing by the surface area of the membrane to yield the velocity of the bulk solution through the membrane as a function of time.

A variety of solutes were tested in the (+1g) orientation, and the resulting osmotic flux measured. Figure 12 shows an overview of these experiments, where the steady state osmotic flux is plotted as a function of solute concentration. Increased concentration results in increased osmotic flux for a given solute.

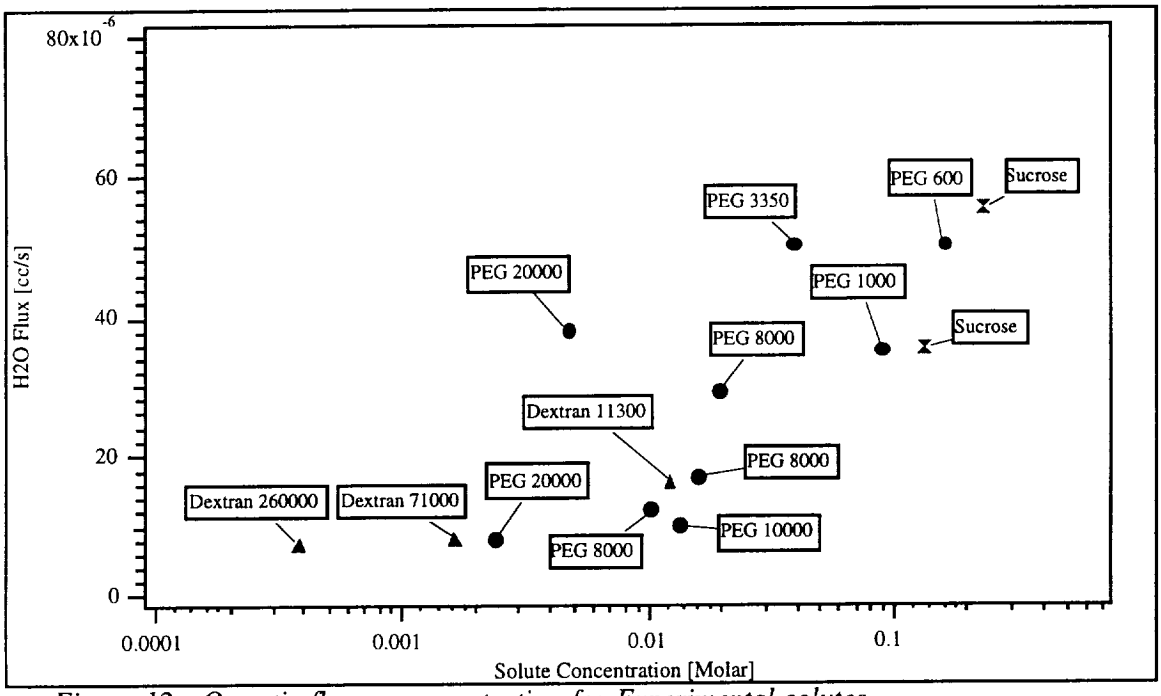

Figure 12 Osmotic flux vs concentration for Experimental solutes

Results From Solute on Bottom (-1g) Gravimetric Configuration

In the solute on bottom configuration, the osmotic solution is present in the lower fluid cell. Osmosis causes lower density solvent (DI water) to pass through the membrane into the higher density solution from the top, and a stably stratified fluid layer is created in association with the membrane. The fluid boundary layer acts to effectively decrease the solute concentration driving potential present at the membrane surface, inhibiting the osmotic process. The concentration gradient present within the fluid boundary layer is visualized by the Fluid Profile Refractometer, and the structure of the boundary recorded as it develops over time. The kinetics of osmosis decrease with time, as is indicated by the decreased flow of solvent through the membrane, and measured by the Volumetric Flow Sensors. Figure 13 shows both raw data and differentiated volumetric flux data from a sucrose on bottom experiment. Solvent is exiting the lower fluid cell, and the level of water decreases with time, causing the osmotic flux to appear as a negative number.

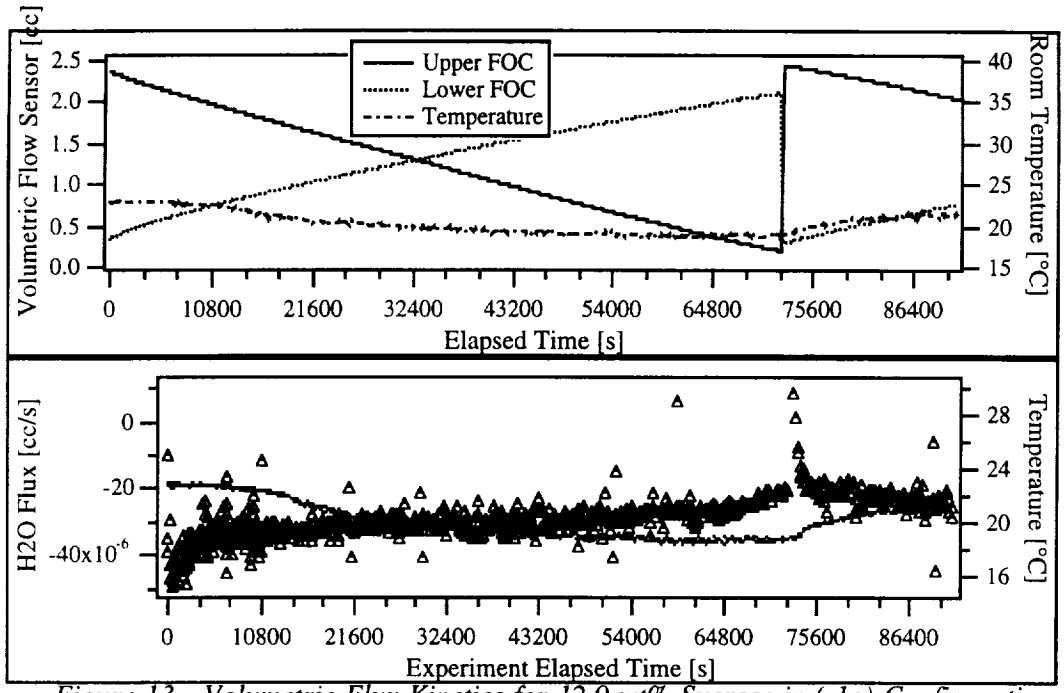

Figure 13 Volumetric Flux Kinetics for 12.9 wt% Sucrose in (-1g) Configuration

Images from the Fluid Profile Refractometer were acquired at intervals during these experiments, and subjected to analysis as described in the data analysis section of this report. Figure 14 shows the boundary layer structure development that was measured in this sucrose osmosis experiments.

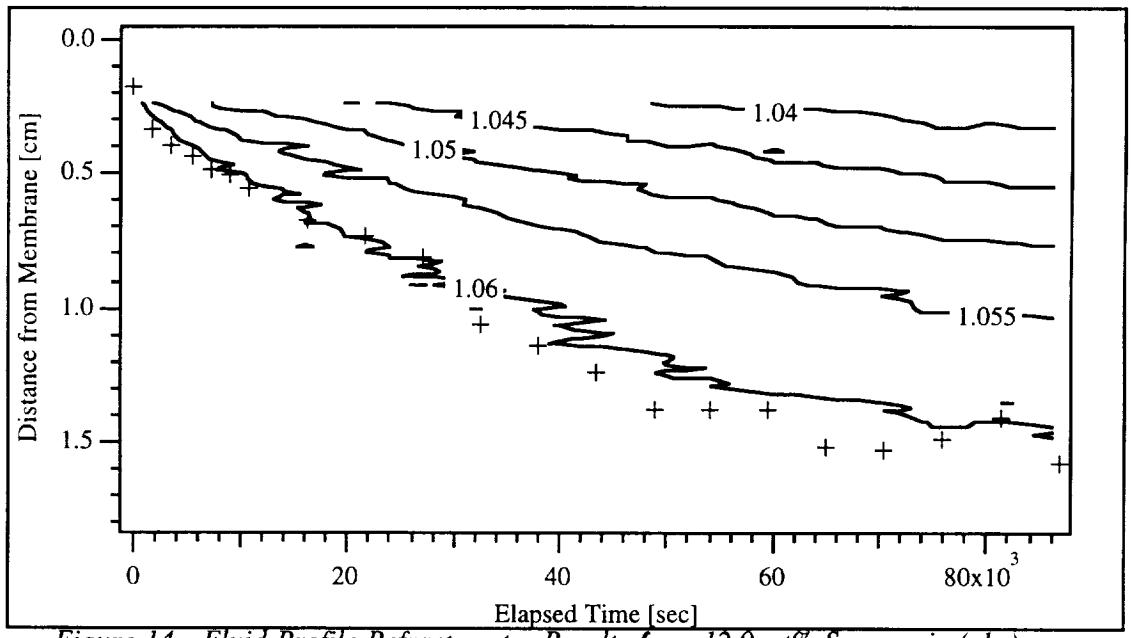

Figure 14 Fluid Profile Refractometer Results from 12.9 wt% Sucrose in (-1g) Configuration Experiment

The crosses shown in the figure indicate the times when images were acquired, and an independent estimate of the total thickness of the fluid boundary layer. The initial conditions for each experiment varied, determined by the solution initial concentration,

weight percent, and density. Examples of the boundary layer structure data are shown in Figure 15, where the fluid boundary layer development is shown to be solute specific. The vertical lines in each of the plots indicate 24 hour periods of time.

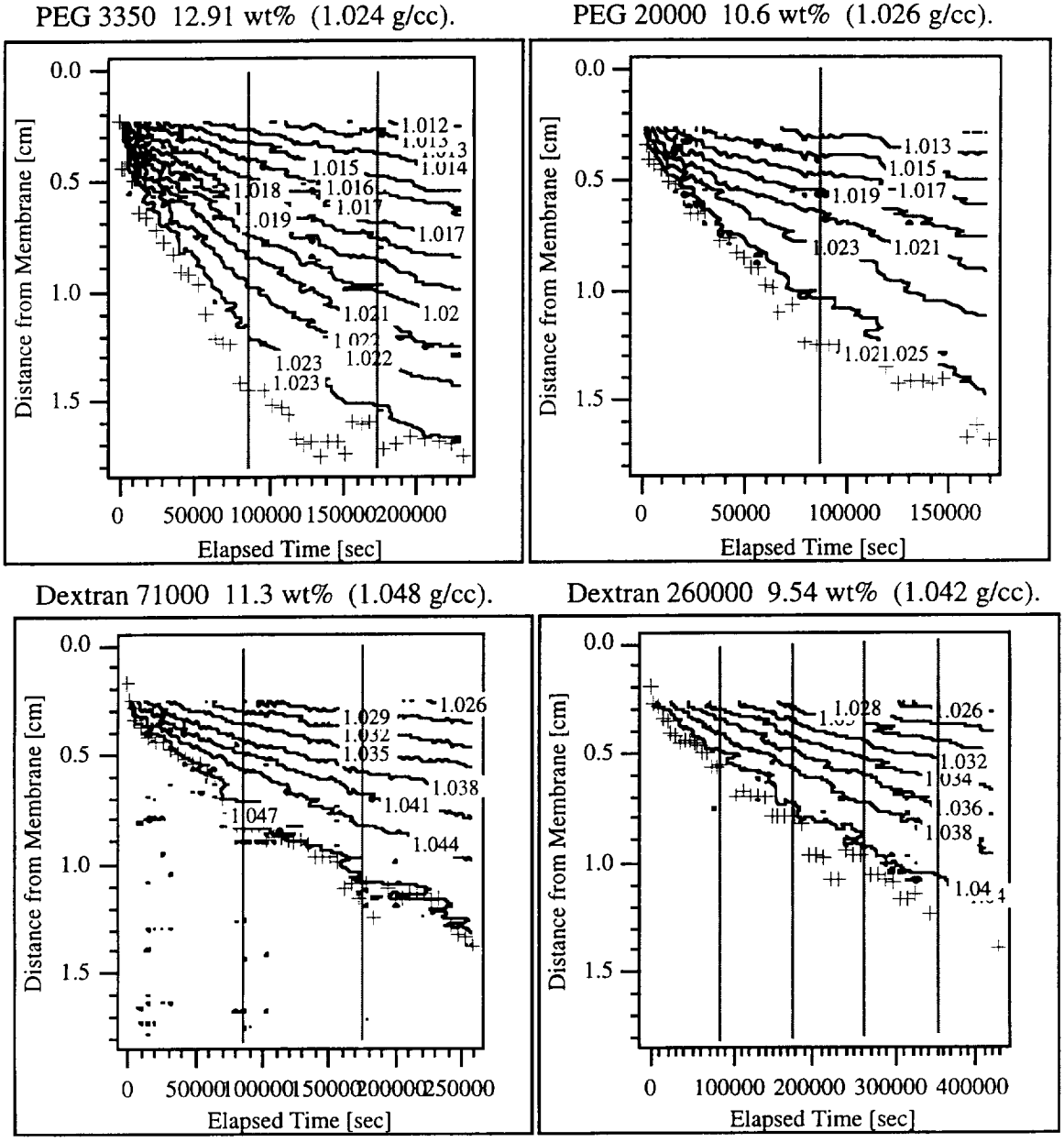

Figure 15 Fluid Profile Refractometer Results for Solutes of Various Molecular Weight in (-1g) Configuration. The initial solution density is indicated in parentheses.

MTP ANALYTICAL MODEL DEVELOPMENT

Two algorithms were developed to model the MTA system, one for each gravimetric orientation (+1g and -1g). The Solute on Top (+1g) model is based on solution bulk properties, and the Solute on Bottom (-1g) model is a finite difference representation where a boundary layer structure develops in association with the membrane.

Solute on Top (+1g) Gravimetric Configuration

The model algorithm developed for the solute on top (+1g) configuration of the MTA is based on stirred tank kinetics, where the fluid is homogeneous at all times, and the bulk properties of the solution determine the osmosis kinetics. Figure 16 shows solvent flux experimental data and model predictions based on this algorithm. The second graph in this figure shows the predicted concentration of the bulk solution as osmosis functions to slowly dilute the solution.

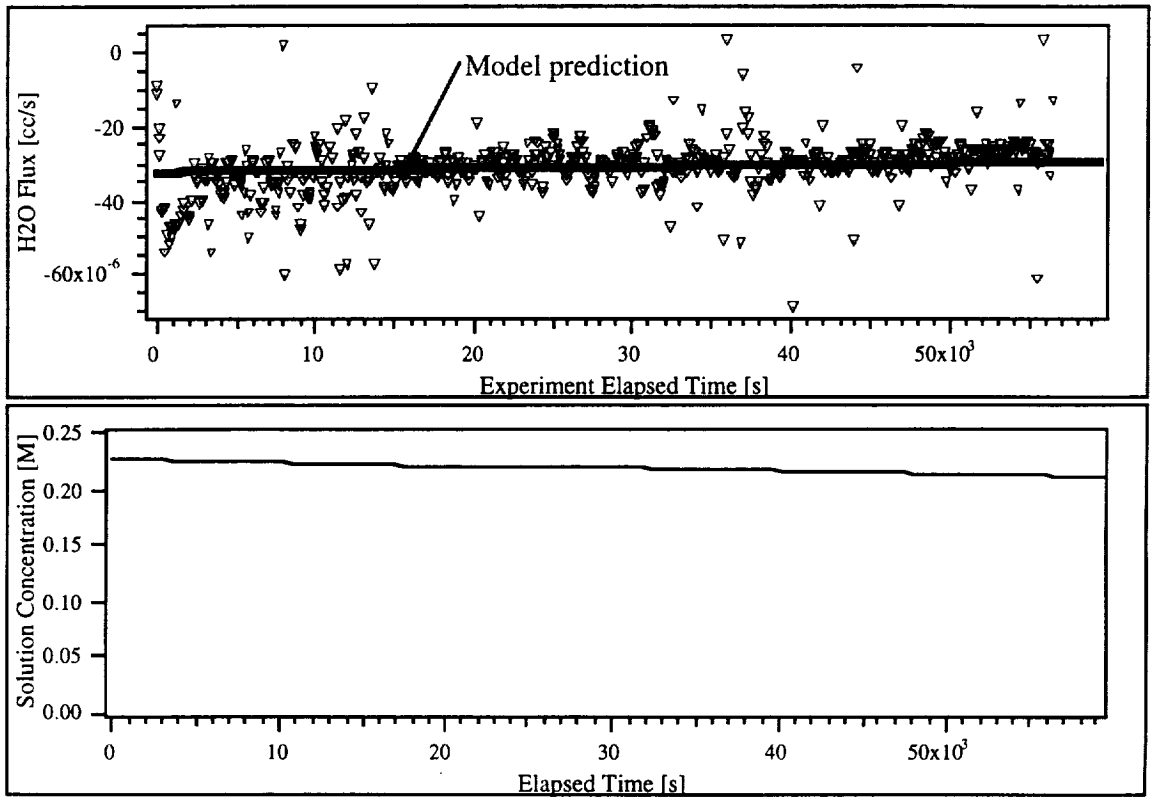

Figure 16 8.0 wt% Sucrose on top (+1g) Osmotic Flux and Model Prediction experimental data (points) and the model predictions (solid line)

Solute on Bottom (-1g) Gravimetric Configuration

The Solute on Bottom (-1g) model is a series of stacked volume elements through which mass transfer occurs. The volume elements remain in a fixed coordinate system provided by the membrane. In this orientation the bulk and diffusive fluxes are in opposite directions, and the fluid structure that develops is a result of the relative interaction between these two opposed fluxes. The bulk flux that enters the initial volume element is determined by the osmotic flow through the membrane, and the diffusive flux is determined by the gradient in solute concentration present in the boundary layer structure. The diffusive flux is modeled by a finite difference approximation to the diffusion equation (marching solution). In the model computation algorithm, these two modes of fluid

movement proceed for a user defined time interval (Δt), and accumulate within the volume element, resulting in a total mixed volume of solution. The specific volume properties of the total solution are determined from the resulting mole fraction, and the volume of solution defined by the volume element is retained within the node. The excess volume is transferred to the adjacent volume element as bulk flux. Figure 17 shows a diagram of this computation algorithm, as used to successively calculate the volume element contents over all nodes for each time step. The membrane is physically excluded from the model, but the osmosis effects are included as the boundary condition present at the initial volume element. The bulk flux of solvent (water) through the membrane is determined as a concentration dependent term that is based on actual (measured) flux in the high convection (+1g) orientation.

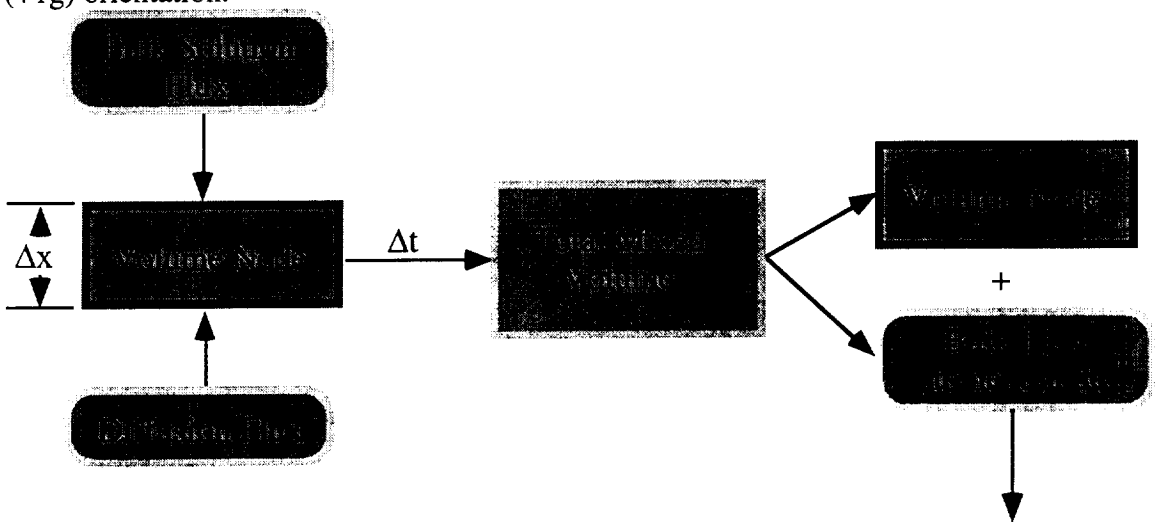

Figure 17 Solute on Bottom (-1g) Model Computation Algorithm

The algorithm also includes the capability to define a solute concentration dependent diffusion coefficient. The model output is generated in a three dimensional graph showing lines of constant fluid density plotted as a function of distance from the membrane and experiment elapsed time. This is the same format as that of the experimental data, and allows direct comparison of experimental results and model predictions.

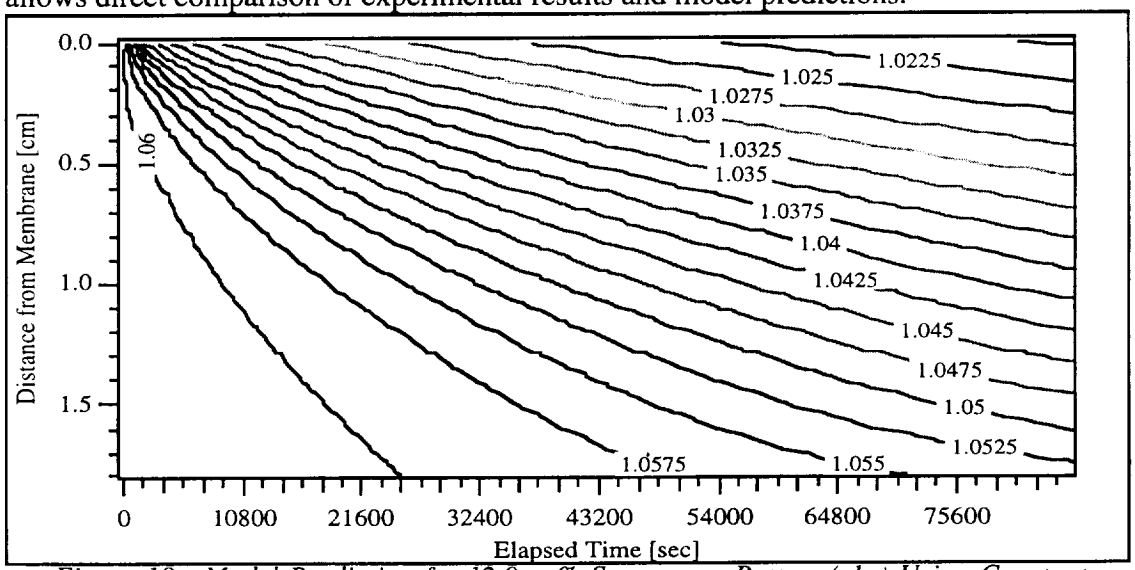

Figure 18 Model Prediction for 12.9 wt% Sucrose on Bottom (-1g) Using Constant $D_{ab}=5.23 * 10^{-6}$ cm²/s

Figure 18 shows the model prediction for 12.9 wt% Sucrose on Bottom (-1g) configuration. This boundary layer structure was generated using a constant diffusion coefficient of 5.23 * 10^{-6} cm^2/s, the literature listed diffusion coefficient value for sucrose in water at infinite dilution (25°C). The predicted fluid structure is different from the observed experimental data, shown previously in Figure 14.

DC-9 MICROGRAVITY EXPERIMENT

Microgravity flight experiments were performed using the NASA/LeRC DC-9 aircraft to test the Fluid Manipulation System (FMS) under microgravity conditions. The experiments were performed during the week of 16 December 1996, and consisted of transferring fluids into and out of two different test cell geometry's within a microgravity environment. Many individual tasks were completed in preparation for these experiments, including development of the test cell hardware and experimental procedures, fabrication of tie down structures, and secure installation of all equipment in the MTP experiment rack. A Safety and Engineering Document was generated and submitted to NASA in preparation for the flights. This document describes the experiment in detail and lists several engineering analyses required for flight. After completion of the experiments, all experiment hardware was returned to LMA from LeRC. All equipment came through the shipping process with no damage.

Two candidate MTP Fluid Optical Cell (FOC) geometry's were developed for this experiment: (1) Quarter Circle cell and (2) Triangular cell. These test cells each have a different internal geometry, and were tested to assess the completeness of filling and draining, and the propensity to trap air bubbles or leave fluid behind during fluid manipulation procedures in microgravity. The cells were sized to allow complete filling/draining within the ~20 seconds of microgravity afforded by each parabolic dive. The filling/draining operations were conducted for a series of fluid pumping rates and fluid port inlet and outlet positions. Red food coloring in deionized water was used in all FMS experiments to visualize the fluid flow patterns. The two MTA computer controlled peristaltic pumps were used to manipulate the fluids during microgravity. Software was developed for control of the experiment such that each experiment could be initiated by a single mouse click at the onset of a parabolic dive. A Video Cassette Recorder (VCR) acquired the video image data showing the completeness of filling/draining. The video system included a character generator that was interfaced to the computer to allow real time display of elapsed time and g-level data directly over the fluid cell images during test operations.

The Test Readiness Review was held at NASA/LeRC at 9:00 AM on 16 Dec. Three microgravity missions (flights) were flown, for a total of 139 parabolas aboard the DC-9 aircraft. The equipment rack and experiment hardware performed well, and good results were obtained. These results will be used to form the basis for microgravity fluid manipulations in the MTP flight experiment. Dramatic differences were seen in fluid cell filling and draining operations in microgravity compared to unit gravity. Figure 19 shows some frames from the experiment video showing examples of the various types of filling and draining scenarios that were observed.

Definite flow patterns were detected within the fluid cells in microgravity. The fluids tended to flow along narrow angles and areas of high curvature. The design of the flight instrument fluid cells can exploit these tendencies using appropriate positioning of inlet and outlet ports, and internal fluid cell geometry that directs the fluid flow in the desired

manner. This should allow the MTP experiment to operate in an autonomous mode, automatically changing fluids between successive experiments.

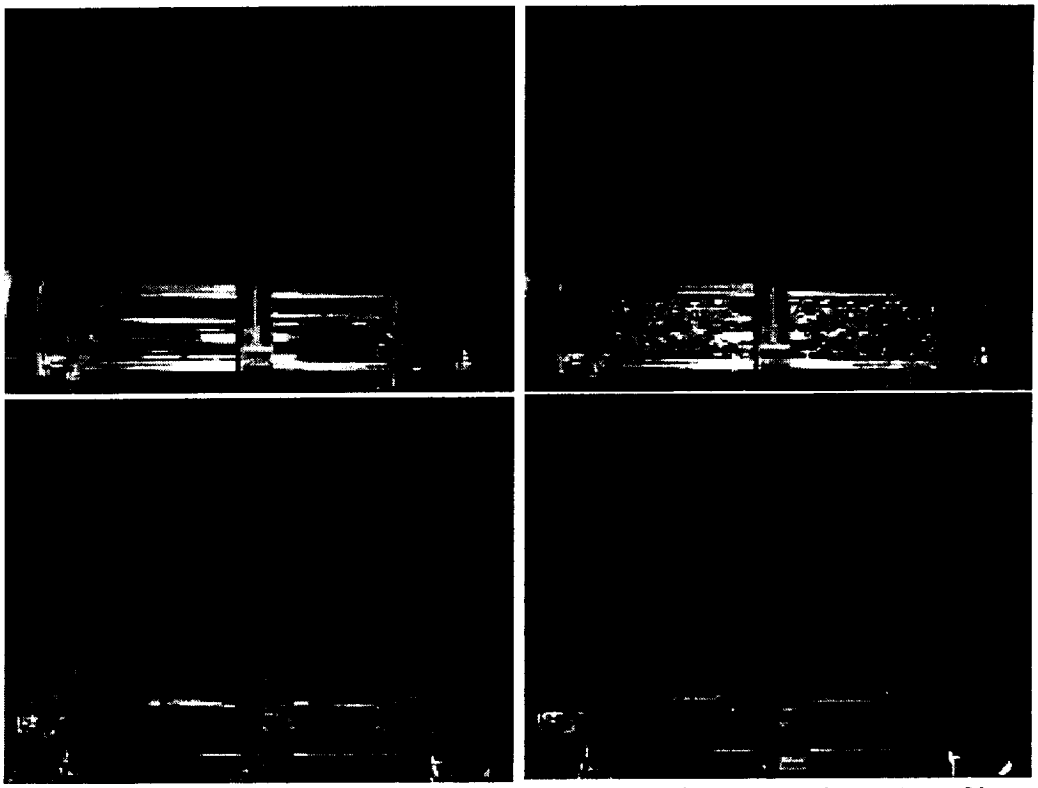

Figure 19 Examples of MTA Fluid Cell Filling and Draining Operations Observed in Microgravity

MICROSENSOR ARRAY DEVELOPMENT

Stanford Research Institute (SRI International) is under contract to fabricate prototype versions of the microsensor arrays that are planned for inclusion in the second generation Membrane Transport experiment (MTA II). This activity is funded by Lockheed Martin Astronautics-Internal Research and Development (LMA-IRAD). The objective of this effort is to develop sensors and instrumentation to measure electrolyte concentrations and driving potential gradients present within the developing fluid boundary layer in the MTA. The microsensor array design includes a series of sensing elements to measure profiles in anion, cation, electrical conductivity, and temperature. Each sensing element is about 50 μm square, and the elements are spaced at intervals ranging from 50 μm to 5,000 μm.

The Ion Sensing Electrodes (ISE) are fabricated using ionophore material that is broadly sensitive to both monovalent and divalent, anions or cations. The ionophore material is deposited in micromachined wells on a ceramic substrate, with electrical contact made using vapor deposited platinum traces. The conductivity and temperature sensors are platinum traces laid down on the ceramic in the appropriate geometry. These traces consist of either insulated serpentine patterns (temperature sensor), or small parallel traces that are in electrical contact with the solution (conductivity cells). The platinum traces that connect to the sensors lead to the edge of the microsensor substrate, and terminate at silver pads to which small wires are bonded for electrical access to the sensors. A polymeric insulation material is used to coat the platinum traces to provide insulation from the experimental solutions.

The microsensor array is being developed in several phases, beginning with individual sensor prototypes. The initial fabrication of the prototype sensors will be used to understand the sensor manufacturing process, and determine the practical minimum spacing for sensors in the array. These results will be used to iterate the design for more advanced versions. The sensor prototypes will also be used to verify the interface electronics for data acquisition, and provide experimental data for proof of the array concept. The prototypes will be evaluated for functionality, and design modifications generated for fabrication of the next phase.

The prototype microsensors were delivered in December 1996. Tests on these single array elements show that most sensors are functional, and meet the preliminary specifications. Some minor technical problems were encountered in the fabrication process associated with the array layout and sealing of insulation material to the ISE ionophore wells. It seems that the insulation material used does not adhere well to the ionophore, and that leaking through this seal occurred on some sensors. A leak of this type in the ISE causes the sensor not to function, as no electrical potential can develop across the ionophore. Additional problems were encountered in wire attachment to the contact pads for transmission of the sensor signals. Wire bonding techniques are available to enable high density connections of this type, but the preliminary technique that was used damaged the original connection pads. Once the pads were damaged, a new layer of silver had to be deposited to form a new connection pad for further wire bonding. Subsequent versions of the sensors will utilize more advanced wire bonding techniques.

These manufacturing problems that were encountered were of the type that was expected, and were solved through evolution of the fabrication process and identification of alternate fabrication materials and techniques. This is the reason that the Microsensor Arrays are being developed in stages, to identify design drivers and allow the manufacturing process to evolve. Further characterization, definition, and development activity is planned for the Microsensor Arrays in CY98 under LMA-IRAD funding.

SCIENCE CONCEPT REVIEW (SCR) PREPARATION

The MTP Science Concept Review (SCR) Panel members were identified, and listed below in Table 1. The SCR presentation was completed, and a dry run held at NASA/MSFC on 5 May 1997. The draft MTP Science Requirements Document (SRD) was completed for inclusion in the SCR presentation package. A preliminary SCR package was sent to each of the SCR panel members, and to the NASA Project Manager and Project Scientist two weeks prior to the SCR. The SCR was held on 13 June 1997, at Lockheed Martin Astronautics in Denver.

Table 1 SCR Panel Members and Affiliation

Professor D.A. Butterfield	University of Kentucky -- Chemistry Dept. (SCR Panel Chair)
Professor R.D. Tilton	Carnegie Mellon University -- Chemical Engineering Dept.
Professor D. Way	Colorado School of Mines -- Chemical Engineering Dept.
Dr. J. Pellegrino	NIST -- Chemical & Physical Properties Division
Professor A.D. Zydney	University of Delaware -- Chemical Engineering Dept.